JOURNAL OF CATALYSIS 138, 675–685 (1992)

Sulfur Poisoning of a Pt/BaK–LTL Catalyst: A Catalytic and Structural Study Using Hydrogen Chemisorption and X-ray Absorption Spectroscopy

M. VAARKAMP,* J. T. MILLER,† F. S. MODICA,† G. S. LANE,† AND D. C. KONINGSBERGER‡,[1]

*Schuit Institute of Catalysis, Eindhoven University of Technology, P.O. Box 513, 5600 MB Eindhoven, The Netherlands; †Amoco Oil Company, Amoco Research Center, 150 W. Warrenville Rd., Naperville, Illinois 60566; and ‡Debye Institute, Laboratory of Inorganic Chemistry, University of Utrecht, P.O. Box 80083, 3508 TB Utrecht, The Netherlands

Received February 19, 1992; revised May 21, 1992

The sulfur poisoning of a Pt/BaK–LTL catalyst has been studied with X-ray absorption spectroscopy and hydrogen chemisorption. The fresh catalyst contained highly dispersed platinum inside the zeolite pores. EXAFS analysis determined a Pt–Pt coordination number of 3.7, suggesting an average platinum cluster size of 5 or 6 atoms, consistent with the TEM and chemisorption data (H/Pt = 1.4). The catalyst was poisoned with H_2S until the dehydrocyclization activity of *n*-hexane decreased to 30% of fresh activity. The first-shell Pt–Pt coordination number increased to 5.5, indicating a growth of the average platinum cluster size to 13 atoms. Hydrogen chemisorption measurements of the poisoned catalyst show a decrease in the H/Pt value to 1.0. The EXAFS data also provide evidence for the presence of sulfur adsorbed on the surface of the platinum particles with a Pt–S bond distance of 2.27Å. The high sensitivity of the Pt/LTL catalyst to poisoning by very low levels of sulfur is attributed to the loss of active platinum surface by adsorption of sulfur and the growth of the platinum clusters. Much of the available platinum surface was found to be capable of chemisorbing hydrogen, but with no activity for dehydrocyclization. Growth of the platinum particle was sufficient to block the pore. In the sulfur-poisoned catalyst, only the sulfur-free platinum atoms exposed through the pore windows remain active. The evidence suggests the location of the sulfur was at or near the metal–zeolite interface. Since both high activity and selectivity require extremely small platinum particles, regeneration of sulfur-poisoned catalysts will require removal of the adsorpted sulfur and restoration of the original particle size.

INTRODUCTION

Platinum supported on LTL zeolite has been found to be a highly active and selective catalyst for dehydrocyclization of straight-chain paraffins, giving high yields of benzene from *n*-hexane (*1*, *2*). Despite its excellent catalytic properties, this catalyst suffers from a high sensitivity to sulfur poisoning (*2*). Therefore, feedstocks with a sulfur content lower than 1 ppm must be used (*3*). Several authors have characterized the Pt/LTL catalyst with techniques including IR (*4*) and TEM (*4–6*), demonstrating the presence of small platinum clusters incorporated within the pores of the zeolite.

In a recent publication (*6*) we described a detailed EXAFS study of a Pt/BaK–LTL catalyst. EXAFS analysis determined a Pt–Pt coordination number of 3.7, suggesting that the average platinum cluster in the zeolite consists of 5 or 6 atoms, consistent with TEM and chemisorption data. EXAFS also detects the platinum-zeolite interface, indicated by Pt–O contributions at 2.14 and 2.71 Å, and a Pt–Ba contribution at 3.8 Å.

Here we report the results from sulfur

[1] To whom correspondence should be addressed.

0021-9517/92 $5.00

poisoning of the same Pt–BaK–LTL catalyst. The objective of this study was to determine the effect of sulfur on the catalyst structure and relate those changes to the catalyst performance. The catalyst was uniformly poisoned with H_2S to a level of 30% of the original activity. The results of our hydrogen chemisorption and EXAFS experiments show that after poisoning, the average platinum particle size increases and that sulfur is bonded to the surface of a metallic platinum particle. In addition to changes in the catalyst activity, sulfur also affects the hydrogenolysis selectivity.

EXPERIMENTAL

Preparation of Catalyst

The K–LTL zeolite was obtained from Linde and found by analysis to contain 6.4 wt% Al, 11.3 wt% K, and 0.04 wt% Na. The zeolite was ion-exchanged with 0.6 *M* barium nitrate for 3 hr at 363 K, washed, and dried at 400 K. The resulting Ba-exchanged zeolite contained 7.4 wt% Ba. The BaK–LTL zeolite was impregnated with tetraamine platinum (II) nitrate to give a sample containing 1.2 wt% Pt. Prior to any further experiments, the sample was reduced at 773 K for 1 hr.

Sulfur Poisoning

After reduction, the sample was cooled to room temperature and transferred to a round-bottom flask. Small quantities of H_2S in H_2 were added to the gas above the catalyst, and the catalyst was rapidly shaken. Following H_2S addition, the catalyst was rereduced at 773 K. The activity of the poisoned catalyst (*n*-hexane conversion, described below) was about 30% of fresh activity. Sulfur levels were too low to be reliably determined by elemental analysis.

Hydrogen Chemisorption

Volumetric hydrogen chemisorption measurements were performed in a conventional glass system at 298 K. Hydrogen was dried by passage over silica. Before measurement of the chemisorption isotherm, the catalyst samples were rereduced for 1 hr (heating rate, 5 K/min) at 773 K and evacuated (10^{-2} Pa) for 1 hr at 773 K. After hydrogen admission at 473 K (hydrogen partial pressure = 93 kPa), desorption isotherms were measured at room temperature. The amount of chemisorbed H_2 was obtained by linear extrapolation of the high-pressure part of the isotherm to zero pressure. Details are given elsewhere (*7*).

Catalyst Testing

The fresh and sulfur-poisoned catalysts were rereduced at 773 K for 1 hr before testing. Catalytic activity and selectivity for n-hexane conversion were evaluated at 673 K using 2.0 g of catalyst in a fixed-bed, continuous-flow, bench-scale reactor. The reactor was operated at atmospheric pressure under flowing hydrogen at 150 ml/min (measured at room temperature and atmospheric pressure). A syringe pump was used to deliver the *n*-hexane (99+% purity) at flow rates of 1.5 and 3.4 g/hr, equivalent to 0.75 and 1.7 WHSV, respectively. Catalytic activity and selectivity were measured 30 min after reactor temperature and reactant flow rates had stablized. Product analyses were conductd by off-line gas chromatography using a 1/8″ × 6′ *n*-octane on Porasil C column.

EXAFS Data Collection

The sample was characterized by EXAFS spectroscopy at the Synchrotron Radiation Source in Daresbury, U.K., Wiggler Station 9.2, using an Si (220) double-crystal monochromator. The storage ring was operated with an electron energy of 2 GeV and a current between 120 and 250 mA. At the Pt L_{III} edge (11564 eV), the estimated resolution was 3 eV. The monochromator was detuned to 50% intensity to avoid the effects of higher harmonics present in the X-ray beam. The measurements were done in the transmission mode. To decrease low- and high-frequency noise as much as possible, each data point was counted for 1 sec and 6 scans were averaged.

The sample was pressed into a self-supporting wafer (calculated to have an absorbance of 2.5) and placed in a controlled-atmosphere cell (*8*), with the sample handled in the absence of air. The sample was heated at a rate of 5 K/min to 723 K in flowing hydrogen (purified and dried) at atmospheric pressure. The sample was held at this temperature for one additional hour, then cooled to room temperature as hydrogen flow was continued. The measurements were done with the sample at liquid nitrogen temperature in the presence of hydrogen at atmospheric pressure.

EXAFS Data Analysis

Data reduction. Standard procedures were used to extract the EXAFS data from the measured absorption spectra (*9, 10*). Normalization was done by dividing the absorption intensities by the height of the absorption edge and subtracting the background using cubic spline routines. The final EXAFS function was obtained by averaging the individual background-subtracted and normalized EXAFS data (6 scans). The standard deviations were calculated for the individual EXAFS data points as a measure of the random error in the final EXAFS function. The EXAFS data analysis is usually performed on an isolated part of the data obtained by an inverse Fourier transformation over a selected range in *r*-space. The isolated EXAFS function was obtained by averaging the inverse Fourier transformations of each individual EXAFS data set (6 scans). The standard deviation calculated from the individual data points of the several isolated EXAFS functions provided a measure of the random error in the average isolated EXAFS function.

Reference data. Data for the phase shifts and backscattering amplitudes were obtained from EXAFS measurements of reference compounds. Pt foil was used as a reference for the Pt–Pt interactions, $Na_2Pt(OH)_6$ for the Pt–O interactions, and H_2PtCl_6 for the Pt–S interactions. The justification for the use of the latter reference is provided by both theoretical (*11*) and experimental (*12*) results. The data analysis procedures used to obtain the reference data for Pt foil and $Na_2Pt(OH)_6$ are described elsewhere (*13*). The determination of the EXAFS reference data for Pt–S was also straightforward, as the first-shell peak in the Fourier transform of H_2PtCl_6 shows no overlap with higher shells.

Data analysis. To reliably determine the parameters characterizing the high Z (Pt) and low-Z (O, S) contributions, multiple-shell fitting in k-space and in r-space was done, with application of k^1 and k^3 weighting. Further optimization of the fit was done by applying the difference file technique and phase- and amplitude-corrected Fourier transforms (*6, 10, 13*).

RESULTS

Catalytic Experiments

The reaction network for conversion of n-hexane over Pt/LTL zeolite catalyst is well established (*2, 14, 15*). The formation of benzene from *n*-hexane is irreversible and occurs via direct 1–6 ring closure. In addition, *n*-hexane reversibly reacts via 1–5 ring closure to form methylcyclopentane, which can ring-open to form methylpentanes. Hydrogenolysis to light gases (C_1–C_5) also occurs. Methylcyclopentane and the methylpentanes were not considered converted products since they can eventually react back to *n*-hexane and subsequently to benzene and light gases. Conversion as we have defined it here, therefore, includes only the irreversible reactions, and represents the sum of hydrogenolysis products (C_1–C_5) plus 1–6 ring closure (benzene). Selectivity to benzene was defined as the yield of benzene divided by the conversion. Hydrogenolysis selectivity was defined as the yield of C_1–C_5 product divided by the conversion.

The results of the catalyst testing are given in Table 1. Relative activity of the fresh catalyst is defined as 1.0. The relative activity of the sulfur-poisoned catalyst has decreased to 0.3. The benzene selectivity

TABLE 1

Dehydrocyclization of *n*-Hexane

	Relative activity	Benzene selectivity
Fresh	1.0	0.90
Sulfur-poisoned	0.3	0.85

decreased from 0.90 to 0.85. The limit of accuracy for the determination of the selectivity is 0.02, indicating a small, but real, effect of sulfur on benzene selectivity.

Hydrogen Chemisorption

Extrapolation to zero pressure yields a value of H/Pt of 1.0 (±0.1) for the sulfur-poisoned catalyst. While the chemisorption method we used systematically gives higher H/Pt values by (about 20%) compared to the conventional procedure (*16, 17*), this method was used in order to enable direct comparison with the correlation of Kip *et al.* (*7*). The hydrogen chemisorption data of the fresh and the sulfur poisoned catalysts are plotted in Fig. 1 together with a correlation derived from Kip *et al.* from several Pt/alumina catalysts.

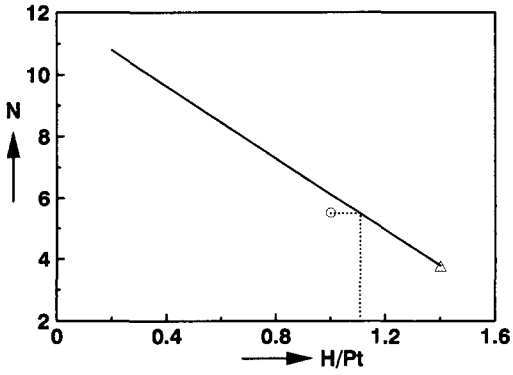

FIG. 1. Combination of hydrogen chemisorption and first-shell Pt–Pt EXAFS coordination number for fresh (triangle) and sulfur-poisoned (circle) Pt/BaK–LTL catalysts. Correlation from Kip *et al.* (*7*) as extended by Vaarkamp *et al.* (*6*).

EXAFS Data Analysis

The raw EXAFS data for the fresh and sulfur-poisoned catalyst are shown in Fig. 2a. The signal to noise ratio is calculated to be 20 at $k = 4$ Å^{-1} and 2 at $k = 12$ Å^{-1}. The larger EXAFS amplitude of the sulfur-poisoned catalyst points to a larger Pt–Pt contribution. The growth of the Pt–Pt contribution of the sulfur-poisoned catalyst is more clearly seen in the Fourier transform (k^1 weighted, Δk: 2.6–12 Å^{-1}) of the data (see Fig. 2b).

The Pt–Pt absorber–backscatterer pair has a nonlinear phase shift and a backscattering amplitude which is strongly dependent on k. This leads to the presence of multiple peaks in a normal, uncorrected Fourier transform of a single Pt–Pt contribution, most clearly seen when a normal uncorrected Fourier transform is weighted with k^2 or k^1. Applying a Pt–Pt phase- and amplitude-correction leads to a single symmetrical Pt–Pt peak in the Fourier transform of a single Pt–Pt EXAFS contribution (Fig. 3).

A Fourier transform with the same weighting and over the same k range was also calculated for the EXAFS data characterizing Pt foil (Fig. 4, dotted line). The magnitude of the Pt foil EXAFS function was adjusted until the first-shell Pt–Pt peak in the Fourier transform scaled with the corresponding peak derived from the sulfur-poisoned catalyst. A comparison of the Fourier transforms (both magnitude and imaginary parts) in Fig. 4 clearly shows the presence of higher Pt–Pt coordination shells in the sulfur-poisoned Pt/BaK–LTL zeolite. As expected, the first Pt–Pt peak in a Pt–Pt phase- and amplitude-corrected Fourier transform of the Pt foil data (Fig. 4, dotted line) appears as a single symmetrical peak. The peaks located at 2.75 Å in the Pt–Pt phase- and amplitude-corrected Fourier transforms of the sulfur-poisoned sample have asymmetrical magnitudes and imaginary parts. This confirms the presence of additional scatterers besides platinum for

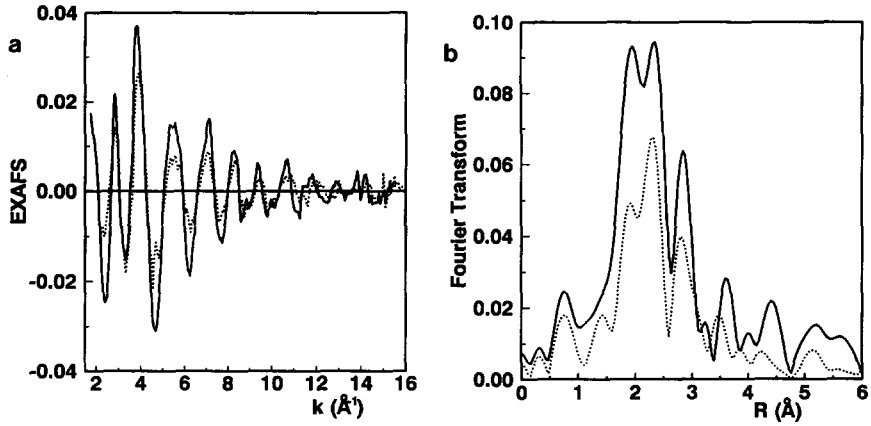

FIG. 2. EXAFS spectrum and Fourier transform of the fresh (-------) and sulfur-poisoned (———) Pt/BaK-LTL catalyst: (a) raw EXAFS spectrum; (b) Fourier transform (magnitude) [k^1, Δk = 2.6–12 Å^{-1}].

both the fresh and sulfur-poisoned catalysts. A full analysis of the EXAFS data of the fresh catalyst showed that the observed differences were due to the presence of neighboring atoms from the metal–zeolite interface (O and Ba) (*6*). The differences between the first peaks in the Fourier transforms as shown in Fig. 4 are caused by the presence of adsorbed sulfur atoms and neighbors from the metal–zeolite interface in the sulfur-poisoned catalyst.

The isolation of the EXAFS contributions giving rise to peaks in the normal Fourier transform between 0.65 and 3.4 Å was carried out by applying an inverse Fourier transform (ΔR: 0.65–3.4 Å) to the data shown in Fig. 2b. First-guess Pt–Pt parameters were obtained by applying a k^3-weighted fit in the range from 6 to 12 Å^{-1} to emphasize the high-Z (viz., Pt–Pt) contribu-

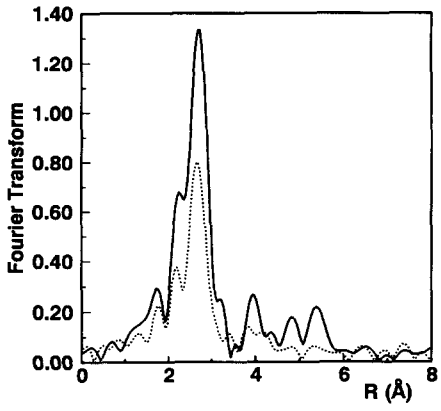

FIG. 3. Fourier transform (magnitude) [k^1, Δk = 3–12 Å^{-1}, Pt–Pt phase- and amplitude-corrected] of EXAFS data for fresh (-------) and sulfur-poisoned (———) Pt/BaK-LTL catalysts.

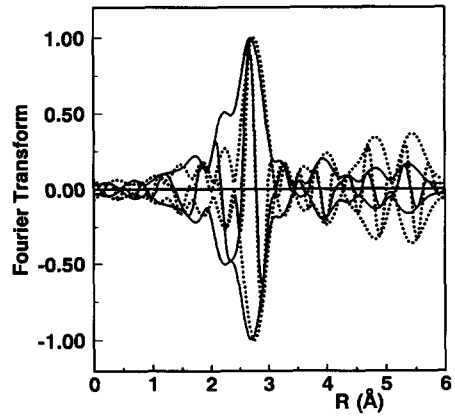

FIG. 4. Fourier transform (magnitude and imaginary part) [k^1, Δk = 3–12 Å^{-1}, Pt–Pt phase- and amplitude-corrected] of EXAFS data for the poisoned Pt/BaK-LTL catalyst (———) and Pt foil (-------). The latter is scaled to the main peak of the FT of the poisoned catalyst.

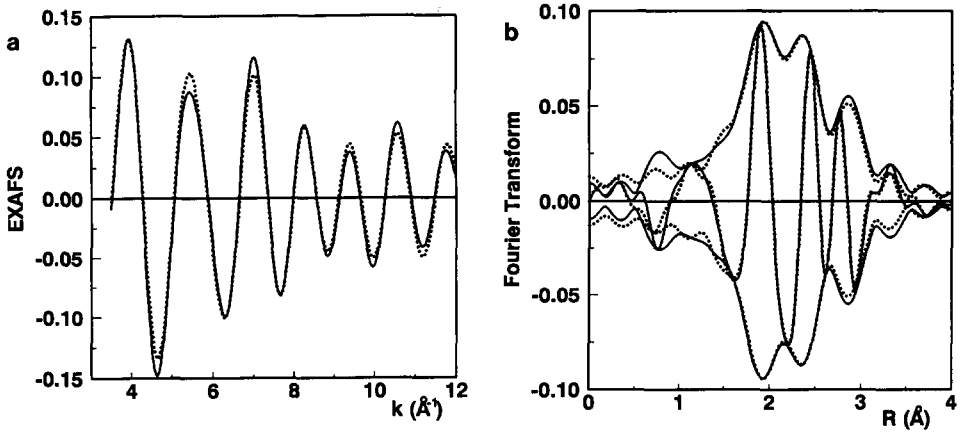

FIG. 5. Isolated EXAFS (———) and fit (-------) for sulfur-poisoned Pt/BaK–LTL catalyst [k^1, Δk = 3.5–12 $Å^{-1}$]: (a) data in k-space; (b) Fourier transform.

tions and deemphasize the low-Z contributions (viz., sulfur and the Pt-zeolite interface). Subtraction of the metal–metal contribution resulted in an EXAFS function which was fitted with contributions characterizing sulfur and the metal–zeolite interface. An iterative fitting procedure (including all contributions) was used to optimize the fits over the whole range of k (3.5–12 $Å^{-1}$), both in k-space and in r-space (using both k^1 and k^3 weighting). A comparison of the fit with the raw data in k-space and in r-space (k^1 weighting) is shown in Fig. 5. The result of this fitting is the identification of three significant contributions (Table 2): a Pt–Pt contribution at 2.75 Å, a Pt–O contribution at 2.69 Å, and a Pt–S contribution at 2.27 Å. The separate contributions to the EXAFS spectrum are shown in Fig. 6. The Pt–S phase-corrected Fourier transform of the difference file obtained by subtracting the Pt–Pt and the Pt–O contributions from the primary EXAFS data (i.e., the inverse Fourier transform of the raw data) is shown in Fig. 6a. The Pt–O contribution is shown in Fig. 6b.

The resulting coordination parameters obtained for the poisoned catalyst together with the results of the fresh catalyst are given in Table 2. The standard deviations given for the sulfur-poisoned catalyst are calculated from the covariance matrix including the actual noise obtained for the Fourier filtered EXAFS function as outlined in the experimental section (EXAFS Data Analysis). The value of the goodness of fit (ε_ν^2) as defined in the "Report on Standards and Criteria in XAFS Spectroscopy" (*18*) was 14.7 with 12 fit parameters and 3.9 degrees of freedom.

DISCUSSION

Structural Results

The EXAFS results clearly show growth of the platinum particles after exposure to sulfur. The Pt–Pt coordination number increases from 3.7 to 5.5. A Pt–Pt coordination number of 5.5 represents, for spherical particles, an average cluster size of approximately 8 Å containing 13 platinum atoms. Consistent with the larger particles, the Debye–Waller factor decreases for the sulfur-poisoned catalyst, and higher Pt–Pt shells are observed which were not present in the fresh catalyst. The first-shell Pt–Pt distance of 2.746 Å and the distances of the observed higher Pt–Pt shells are consistent with the presence of metallic platinum particles.

In addition to the particle growth, EXAFS

TABLE 2

EXAFS Results for Fresh and Sulfur-Poisoned Pt/BaK–LTL Fitted Parameters with Standard Deviations[a]

Backscatterer	N	R(Å)	$\Delta\sigma^2$ (Å^2 × 10^{-4})	ΔE_0 (eV)
Pt				
Fresh	3.7 ± 0.3	2.75 ± 0.02	32 ± 5	1.4 ± 0.5
Sulfur-poisoned	5.5 ± 0.3	2.746 ± 0.002	27 ± 4	2.4 ± 0.5
O				
Fresh	0.6 ± 0.1	2.14 ± 0.03	67 ± 10	1.8 ± 0.5
Fresh	1.1 ± 0.2	2.71 ± 0.03	95 ± 20	2 ± 1
Sulfur-poisoned	1.1 ± 0.3	2.70 ± 0.03	40 ± 34	4 ± 2
Ba				
Fresh	1.4 ± 0.2	3.76 ± 0.05	90 ± 20	6.6 ± 1.0
Sulfur-poisoned	—	—	—	—
S				
Fresh	—	—	—	—
Sulfur-poisoned	1.2 ± 0.1	2.27 ± 0.01	34 ± 9	5 ± 2

[a] Standard deviations for sulfur-poisoned catalyst calculated from a full statistical analysis including the standard deviation at each data point. Estimates for fresh catalyst were made from estimates of the signal/noise present in the scans.

clearly shows the presence of sulfur chemisorbed on the outer surface of the platinum particle. The observed platinum–sulfur distance of 2.27Å is shorter than the distances for bulk PtS (2.31 Å) (*19*) and PtS_2 (2.40 Å), which is consistent with sulfur chemisorbed on a metallic particle. For example, LEED measurements of sulfur chemisorbed on Ni single crystals indicate that neither bulk nor surface nickel sulfides are formed, and that the Ni–S bond distance is 0.1 to 0.2 Å shorter than observed for Ni_3S_2, NiS_2, and α-NiS (*20, 21*). Also, a longer Pt–Pt distance at 3.54 Å, such as would be present in bulk PtS_2, is not observed. The measured coordination number of 1.2 indicates that each platinum atom sees, on average, slightly more than one sulfur atom in its first coordination shell. Since sulfur tends to adsorb on platinum faces in hollow sites, this coordination number indicates a surface S/Pt atomic ratio of about 0.4.

The presence of sulfur on the surface of the platinum particles has a pronounced effect on the structure of the platinum zeolite interface: both the Pt–O distances and coordination numbers are affected. In the fresh catalyst two Pt–O distances are observed, one at 2.14 Å and one at 2.71 Å. The distance at 2.14 Å is believed to be due to zero-valent, interfacial platinum supported on an oxide surface. The longer distance of 2.71 Å is believed to be due to the presence of hydrogen between the platinum cluster and the zeolite oxide surface (*22*). In the sulfur-poisoned Pt/BaK–LTL catalyst, the shorter Pt–O distance of 2.14 Å is no longer observed. In addition, the total Pt–O coordination number decreases from 1.7 in the fresh catalyst to 1.0 for the sulfur-poisoned catalyst. This decrease in the contribution from the platinum–zeolite interface is consistent with an increased platinum particle size. It is also possible that the adsorbed sulfur is at or near the platinum–zeolite interface, reducing the amount of interfacial oxygen atoms in the first coordination shell.

In addition to changes in Pt–O contributions, the Pt–Ba distance observed for the fresh catalyst could not be detected in the

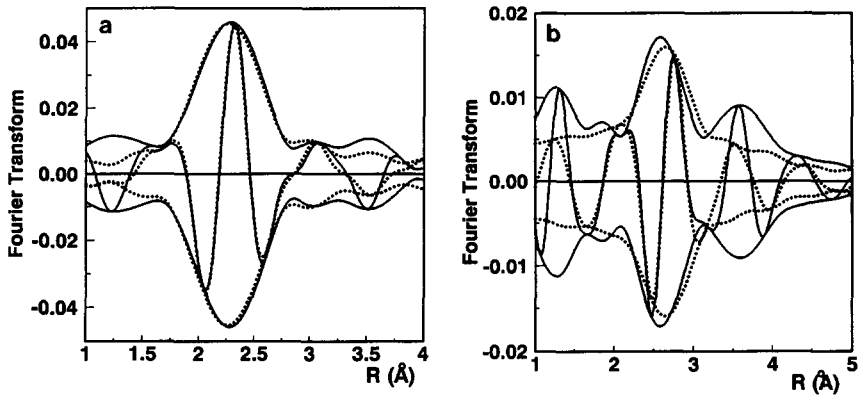

FIG. 6. Fourier transform [k^1, Δk = 3.5–9 $Å^{-1}$] of difference files: (a) Isolated EXAFS minus the calculated Pt–Pt and Pt–O contributions (———) and calculated Pt–S contribution (-------) [both Pt–S phase-corrected). (b) Isolated EXAFS minus the calculated Pt–Pt and Pt–S contributions (———) and calculated Pt–O contribution (-------) [both Pt–O phase-corrected].

sulfur-poisoned catalyst. This result also indicates a lower contribution from the platinum–zeolite interface.

In summary, the sulfur-poisoned catalyst has larger platinum particles than the fresh catalyst. The platinum particle, however, remains metallic in character and does not form platinum sulfide. Rather, the short Pt–S distance determined by EXAFS is consistent with sulfur chemisorbed on the surface of a metallic platinum cluster. Finally, the weakened Pt–O contribution and the absence of a Pt–Ba contribution suggests that the sulfur is located at the metal–zeolite interface.

Chemisorption and Catalytic Performance

As pointed out above, sulfur poisoning increased the average platinum particle size from 5–6 atoms to about 13 atoms. The fresh catalyst had an average coordination number of 3.7 and an H/Pt of 1.4, while the poisoned catalyst had an average coordination of 5.5 and an H/Pt of 1.0. Based on the previous correlation of particle size and hydrogen chemisorption (*6, 7*), a sulfur-free platinum catalyst with a coordination number of 5.5 would be expected to have a H/Pt value of 1.1 (see dotted line in Fig. 1). Thus, of the 0.4 H/Pt difference between the fresh and sulfur-poisoned catalyst, 0.3 H/Pt can be attributed to the particle growth. Only the remaining 0.1 H/Pt is due to coverage by sulfur. This difference is at or near the experimental accuracy of the technique. Assuming sulfur occupies a three fold coordination site (*23, 24*), the first-shell Pt–S coordination number of 1.2 corresponds to about 0.4 sulfur atoms per surface platinum atom. Thus, while the EXAFS results show that the sulfur is chemisorbed on the platinum surface, nearly all of the surface platinum atoms remain capable of chemisorbing hydrogen.

With a Pt–S coordination number of 1.2, one might expect the catalyst to have little or no activity. However, since 30% of the fresh activity remained, it is clear that much of the platinum surface is not poisoned by sulfur. The unexpectedly high hydrogen chemisorption, coupled with the higher than expected activity, strongly suggests that sulfur is not evenly distributed over the platinum surface, but rather, is concentrated at or near the metal–zeolite interface, leaving most of the exposed platinum surface unpoisoned. The location of the sulfur at the metal–zeolite interface is also consistent

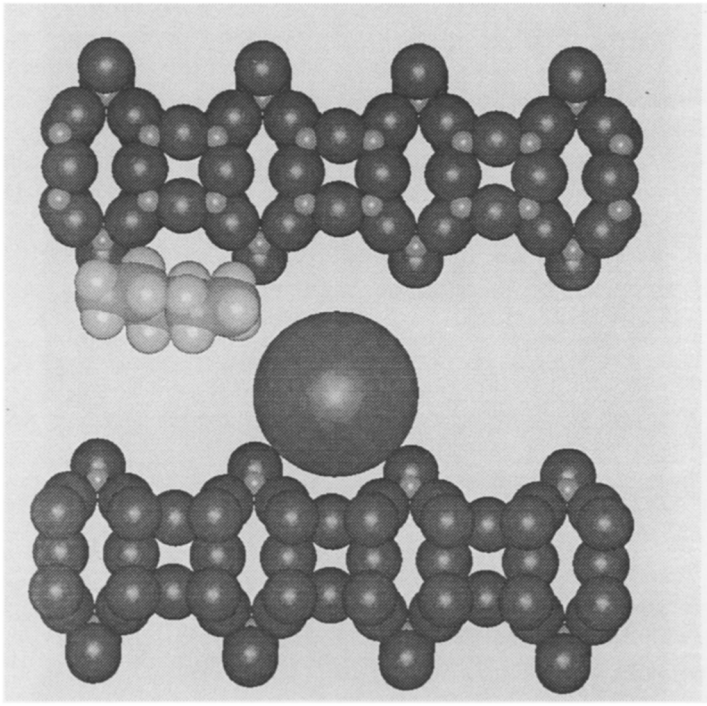

FIG. 7. Molecular model of LTL zeolite channel (parallel to *c*-axis) containing platinum cluster represented by an 8-Å sphere. Sulfur and zeolite cations omitted for clarity. Molecular of *n*-hexane shown to scale.

with the observed weakening of the Pt–O and Pt–Ba interactions detected by EXAFS.

While the available platinum surface (as measured by hydrogen chemisorption) decreased by only 25%, the catalytic activity decreased by 70%. Therefore, a large fraction of the platinum surface remains capable of chemisorbing hydrogen, but is inactive for hexane dehydrocyclization. While ensemble size effects cannot be ruled out, these results suggest that the larger platinum particles may partially block the zeolite channels. A 13-atom cluster is approximately 8 Å in diameter, nearly filling the zeolite channel (11 Å at its widest point) (see Fig. 7). It is evident from Fig. 7 that the space between the platinum particle and the opposite wall of the zeolite channel is large enough to allow chemisorption of hydrogen to the platinum surface atoms but too small to admit the larger hexane molecule.

While there was a large decrease in catalytic activity, the selectivity to benzene decreased from 0.90 for the fresh catalyst to 0.85 in the sulfur-poisoned catalyst. Selectivity to light gases (C_1–C_5), i.e., hydrogenolysis selectivity, increased from 0.10 in the fresh catalyst to 0.15 in the sulfur-poisoned catalyst—a 50% increase in hydrogenolysis selectivity due to sulfur poisoning. Hydrogenolysis is well known to be a structure-sensitive reaction (the specific activity is particle size dependent) (*25, 26*). The observed increase in hydrogenolysis selectivity may, therefore, be attributed to the increase in the platinum particle size. This, in turn, implies a larger ensemble requirement for hydrogenolysis as compared to dehydrocyclization. Thus, as the particle size grows,

larger ensembles are formed, favoring hydrogenolysis over dehydrocyclization. It is worth noting that sulfur-poisoning of large metallic particles generally results in a *decrease* in hydrogenolysis selectivity, generally attributed to the loss in the number of large, unpoisoned ensembles (*27, 28*). However, suppression of hydrogenolysis by sulfur passivation has been reported only for catalysts with much larger metallic particles.

CONCLUSION

Poisoning of Pt/BaK–LTL catalysts by sulfur results in a growth in the platinum particles. Bulk platinum sulfides are not formed—the platinum remains metallic with surface chemisorbed sulfur. Sulfur also appears to disrupt the metal–zeolite interface and the evidence suggests preferential location of sulfur at the metal–zeolite interface. Backscattering contributions from the zeolite surface oxygen are reduced and barium contributions are no longer observed. Also, the long Pt–O contribution due to interfacial hydrogen is no longer observed. The disruption of the platinum–zeolite interface by sulfur may also contribute to the observed growth in the platinum particle size.

The extreme sensitivity of Pt/LTL catalysts poisoning by low levels of sulfur appears to be due, at least in part, to the growth of the platinum particles. Poisoning of the platinum surface by sulfur appears to be qualitatively similar to poisoning by sulfur in nonzeolitic catalysts. The promotion of particle growth by sulfur provides an additional means by which active metal surface is lost. As the platinum particle size approaches the size of the zeolite channel, much of the platinum surface is no longer accessible to reactants.

The growth of the platinum particle also effects the reaction selectivity. Hydrogenolysis selectivity increases on the larger particles, resulting in lower benzene selectivity.

The results of this study indicate that successful regeneration of sulfur-poisoned Pt/LTL catalysts requires both the removal of sulfur from the catalyst and restoration of the original small platinum particle size. At the same time, the platinum particles must remain with the zeolite channels.

REFERENCES

1. Bernard, J. R., *in* "Proceedings, 5th International Zeolite Conference" (L. V. C. Rees, Ed.), p. 686. Heyden, London, 1980.
2. Hughes, T. R., Buss, W. C., Tamm, P. W., and Jacobson, R. L., "Proceedings, 7th International Zeolite Conference" (Y. Murakami, A. Iijima, and J. W. Ward, Eds.), p. 725. Kodansh, Tokyo, 1986.
3. Buss, W. C., Field, L. A., and Robinson, L. C., U.S. patent 4,456,527 (1984).
4. Besoukhanova, C., Guidot, J., Barthomeuf, D., Breysse, M., and Bernard J., *J. Chem. Soc. Faraday Trans. 1* **77,** 1595 (1981).
5. Rice, S. B., Koo, J. Y., Disko, M. M., and Treacy, M. M. J., *Ultramicroscopy* **34,** 108 (1990).
6. Vaarkamp, M., van Grondelle, J., Miller, J. T., Sajkowski, D. J., Modica, F. S., Lane, G. S., Gates, B. C., and Koningsberger, D. C., *Catal. Lett.* **6,** 369 (1990).
7. Kip, B. J., Duivenvoorden, F. B. M., Koningsberger, D. C., and Prins, R., *J. Catal.* **105,** 26 (1987).
8. Kampers, F. W., Maas, T. M. J., van Grondelle, J., Brinkgreve, P., and Koningsberger, D. C., *Rev. Sci. Instrum.* **60,** 2645 (1989).
9. Cook, J. W., Jr., and Sayers, D. E., *J. Appl. Phys.* **52,** 5024 (1981).
10. van Zon, J. B. A. D., Koningsberger, D. C., van't Blik, H. F. J., and Sayers, D. E., *J. Chem. Phys.* **12,** 5742 (1985).
11. Teo, B. K., and Lee, P. A., *J. Am. Chem. Soc.* **101,** 2815 (1979).
12. Lengeler, B. J., *J. Phys., Colloq.* **C8(1),** 75 (1986).
13. Kampers, F. W. H., PhD thesis, Eindhoven University of Technology, Eindhoven, 1989.
14. Lane, G. S., Modica, F. S., and Miller, J. T., *J. Catal.* **129,** 145 (1991).
15. Tamm, P. W., Mohr, D. H., and Wilson, C. R., *in* "Catalysis 1987" (J. H. Ward, Ed.) p. 335. Elsevier, Amsterdam, 1988.
16. Larsen, G., Haller, G. L., *Catal. Lett.* **3,** 103 (1989).
17. Ostgard, D. J., Kustov, L., Poeppelmeier, K. R., Sachtler, W. M. H., *J. Catal.* **133,** 342 (1992).
18. Lytle, F. W., Sayers, D. E., and Stern, E. A., *Physica B* **158,** 701 (1989).
19. Heegemann, W., Meister, K. H., Bechtold, E., and Hayek, K., *Surf. Sci.* **49,** 161 (1975).

20. Demuth, J. E., Jepsen, D. W., and Marcus, P. M., *Phys. Rev. Lett.* **32,** 1182 (1974).
21. Marcus, P. M., Demuth, J. E., and Jepsen, D. W., *Surf. Sci.* **53,** 501 (1975).
22. Kampers, F. W. H., Koningsberger, D. C., *Faraday Discuss. Chem. Soc.* **89,** 137 (1990).
23. Bartholomew, C. H., Agrawal, P. K., and Katzer, J. R., *Adv. Catal.* **31,** 135 (1982).
24. Martin, G. A., *Catal. Rev.-Sci. Eng.* **30(4),** 519 (1988).
25. Boudart, M., and Djega-Mariadassou, G., *in* "Kinetics of Heterogeneous Catalytic Reactions" (J. M. Prausnitz, L. Brewer, Eds.). Princeton Univ. Press, Princeton, NJ, 1984.
26. Che, M., and Bennett, C. O., *Adv. Catal.* **36,** 55 (1989).
27. Hayes, J. C., Mitsche, R. T., Pollitzer, E. L., and Homeier, E. H., *Prepr. Am. Chem. Soc. Div. Pet. Chem.* **19,** 334 (1974).
28. Shum, V. K., Butt, J. B., and Sachtler, W. M. H., *J. Catal.* **96,** 371 (1985).